

Resonance effects in the carrier-tunneling dynamics in asymmetric coupled quantum wells

Ph. Roussignol*

Laboratorio Europeo di Spettroscopia Non-Lineari, Largo Enrico Fermi 2, 50125 Firenze, Italy

A. Vinattieri, L. Carraresi, and M. Colocci

Dipartimento di Fisica and Laboratorio Europeo di Spettroscopia Non-Lineari, Largo Enrico Fermi 2, 50125 Firenze, Italy

A. Fasolino

Scuola Internazionale Superiore di Studi Avanzati, Via Beirut 2-6, 34100 Trieste, Italy

(Received 6 May 1991)

We present a detailed experimental study of the tunneling times, after picosecond excitation, of electrons and holes in a large set of unbiased GaAs/Al_xGa_{1-x}As asymmetric double-quantum-well structures, pointing out the role played by resonances in the tunneling process. In particular, fast hole tunneling is found when the quantum wells show band alignment both at $k_{\parallel}=0$ and at $k_{\parallel}\neq 0$. Referring to electrons, a resonance is found in the tunneling time, which corresponds to phonon-assisted processes. Experimental data at high excitation intensity are also reported, suggesting band-filling effects in the wider well.

INTRODUCTION

After the pioneering works of Esaki and Tsu,¹⁻³ a great deal of activity has been devoted, in recent years, to the study of carrier tunneling both in double barrier and asymmetric double-quantum-well heterostructures (ADQW), due to the interest that such structures have for device applications, on the one hand, and for the basic quantum-mechanical aspects, on the other.

However, in spite of the large number of papers on the subject, some fundamental questions do not yet seem clearly understood. In fact, while a large amount of experimental work has been devoted to both nonresonant and resonant electron tunneling,⁴⁻¹⁰ definitively less is known in the case of hole tunneling. In particular the role played in ADQW's by resonances between hole states in the two wells is still controversial and no consensus has yet been reached on the question of whether band-mixing effects between heavy- and light-hole states are important in determining the tunneling times.¹¹⁻¹³ Nor is the question definitely clarified of whether exciton transfer as a whole, rather than electron and/or hole tunneling, is observed in these structures.¹⁴⁻¹⁶

In this paper we present an experimental study of the effects of band alignment on the tunneling times in a large set of unbiased GaAs/Al_xGa_{1-x}As ADQW's by using picosecond time-resolved photoluminescence spectroscopy. For fixed barrier thickness, we find a significant reduction of the electron-tunneling time out of the narrow well as soon as the energy mismatch between the ground states in the conduction band of the two wells becomes larger than the LO phonon energy. We also find fast hole tunneling (≤ 100 ps) not only when the quantized heavy-hole levels are approximately resonant in the two wells but also whenever a resonance is present be-

tween heavy- and light-hole states induced by band-mixing effects at $k_{\parallel}\neq 0$.

The paper is organized as follows: a brief description of the samples and the experimental apparatus is given in Sec. I. The experimental results, together with the set of rate equations used for deducing the tunneling times from the time-resolved measurements, are presented in Sec. II. A discussion of the experimental results for the electron- and hole-tunneling times is given in Secs. III A and III B, respectively. The results of a calculation of the hole dispersion and wave functions in the presence of band mixing are also presented in Sec. III B. Finally, conclusions are given in the final section.

I. SAMPLES AND EXPERIMENT

The samples were undoped GaAs/Al_xGa_{1-x}As ADQW heterostructures grown by molecular-beam epitaxy on a Si-doped (001) oriented GaAs substrate with an aluminum content in the Al_xGa_{1-x}As alloy ranging from 0.28 to 0.33. A complete description of the whole set of samples investigated is found in Ref. 17.

In the following, we will denote the samples with the notation "sample ($L_W/L_B/L_N$)," where L_W , L_N , L_B give the thickness of the wide well (WW), the narrow well (NW), and the barrier, respectively.

As stressed by Alexander *et al.*,⁸ the advantage of dealing with samples consisting of only one ADQW structure, like ours, is in removing any possible contribution to the tunneling process from Bloch-like transport and in avoiding thickness fluctuations in the QW's as well as in the barriers.

In order to characterize the samples, cw photoluminescence (PL) and photoluminescence excitation (PLE) spectra have been performed using a He-Ne laser and a

Ti:sapphire tunable laser pumped by a 5 W Ar⁺ ion laser. The spectra were recorded by a standard photon-counting system after dispersion of the luminescence through a 0.6 m double spectrometer. PL time-resolved measurements have been performed exciting the luminescence with a picosecond dye laser synchronously pumped by the second harmonic of a Nd:YAG mode-locked laser; 5 ps pulses have been used, with the wavelength varying in the range 750–820 nm, at a repetition rate of 76 MHz. The excitation density was varied from below $5 \times 10^{10} \text{ cm}^{-2}$ up to $5 \times 10^{12} \text{ cm}^{-2}$. The PL signal was dispersed through a 0.22 m double spectrometer (1 meV resolution) and detected by a synchroscan streak camera with an overall time resolution of 20 ps. All the measurements have been performed at 4 K, keeping the sample fully immersed in a liquid-helium cryostat.

II. EXPERIMENTAL RESULTS

A. cw measurements

A schematic diagram of the relevant energy levels of the heterostructures investigated is reported in Fig. 1. In the following we will always report the values of L_W , L_B , L_N , as those obtained from a best fit of the PLE peak energies using a standard model based on the effective-mass approximation^{18,19} for the coupled wells; good agreement with the PLE spectra has been obtained for values typically 10% lower than the nominal ones, as also found by other authors.^{4,20}

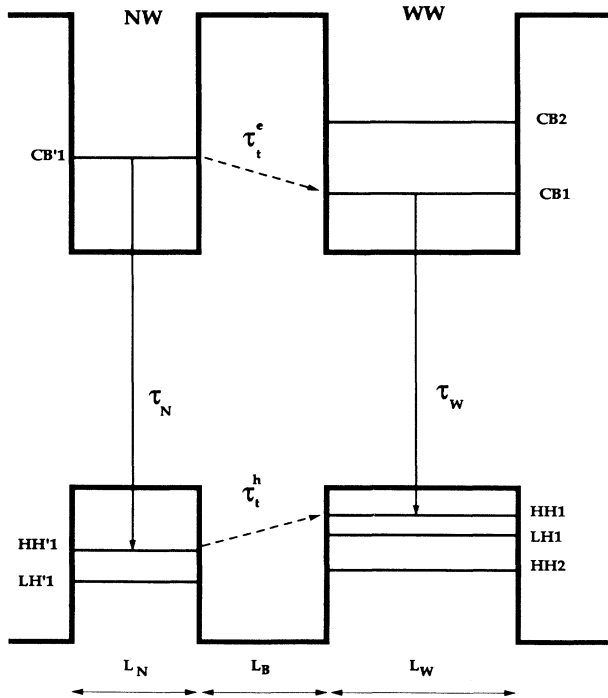


FIG. 1. Schematic diagram of the relevant energy levels in an asymmetric double-quantum-well structure.

In Fig. 2 typical PL and PLE spectra are reported for samples $(87 \text{ \AA})/(70 \text{ \AA})/(31 \text{ \AA})$ and $(87 \text{ \AA})/(20 \text{ \AA})/(31 \text{ \AA})$, only differing in the barrier thickness. In both cases a comparison between the PL and the PLE spectra unambiguously shows that tunneling occurs from the narrow to the wide well. In fact clearly resolved structures corresponding to the heavy and light exciton transition CB'1-HH'1 and CB'1-LH'1 from the narrow well are present when detecting the luminescence, in the PLE spectrum, on the low-energy side of the CB1-HH1 transition from the wide well. However, the PL intensity from the narrow well is strongly dependent on the sample; no signal is detected for the sample with $L_B = 20 \text{ \AA}$ even when the excitation intensity is increased to 140 W cm^{-2} , indicating that carrier tunneling is a very efficient process in emptying the narrow well. Note the absence of a significant

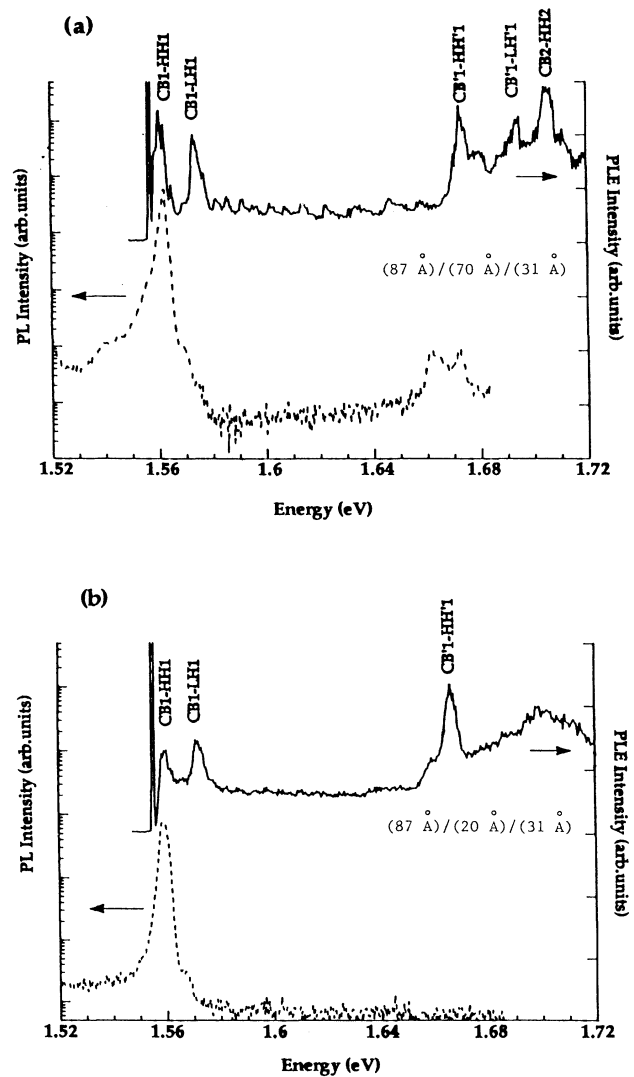


FIG. 2. Comparison between the PL and PLE spectra of samples differing only in the barrier thickness: (a) PL (dotted line—logarithmic scale) and PLE (solid line—linear scale) of sample $(87 \text{ \AA})/(70 \text{ \AA})/(31 \text{ \AA})$; (b) PL (dotted line—logarithmic scale) and PLE (solid line—linear scale) of sample $(87 \text{ \AA})/(20 \text{ \AA})/(31 \text{ \AA})$.

Stokes shift between the PL and PLE spectra, indicating recombination of free excitons and good quality of the heterostructure interfaces.

B. Time-resolved measurements

We report in Fig. 3 typical decay curves of the photoluminescence in an ADQW structure. First, we always observe a fast monoexponential decay for the PL from the narrow well [Fig. 3(a)], the relevant time constant being strongly dependent on the barrier width and the energy mismatch between the ground electronic levels of the two wells.

On the contrary, the decay of the PL from the wide well is very sensitive to the excitation wavelength [Figs. 3(b) and 3(c)]. In fact, while a monoexponential decay with constant τ_W is observed for resonant excitation of the transition CB1-LH1 when only the wide well is excited, a nonexponential decay is observed when both wells are excited at the same time together with a non-negligible rise time dependent on both L_N and L_B . Moreover, a strong modification of the PL decay curve from the wide well has been observed when increasing the excitation intensity.

The PL decay from both wells, after excitation at the CB'1-LH'1 transition, is reported in Figs. 4(a) and 4(b) for different excitation intensities. As it is easily seen, monoexponential decays are observed for the exciton recombination from the narrow well independently from the excitation intensity. On the contrary, a strong modification of the PL decay from the wide well is observed as the excitation intensity is increased from 1 to 140 W cm^{-2} . In particular, referring to Fig. 4(b), while a single rise time is observed at low intensity, two time con-

stants in the PL rise time seem to be involved (the second one much longer than the first one) when considering the highest intensity. This effect is clearly observed in the case of the wide well; on the contrary, only minor modifications are observed for the PL from the narrow well [Fig. 4(a)].

Two possible explanations of this effect may be invoked. On one hand, a slower tunneling of holes with respect to electrons may lead to a spatial charge separation in the heterostructure that gives rise to an electrostatic field and therefore to significant band bending. On the other hand, band filling of the levels of the wide well may occur as the excitation intensity increases. Nevertheless, in our case, the observation of strong modifications of the exciton decay from the wide well

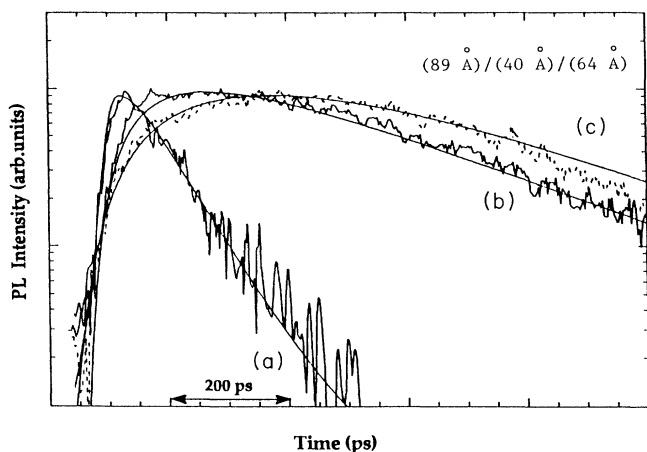


FIG. 3. Typical PL decay curves of sample $(89 \text{ \AA})/(40 \text{ \AA})/(64 \text{ \AA})$: (a) PL decay from the narrow well after excitation of the transition CB'1-LH'1; (b) PL decay from the wide well after excitation of the transition CB1-LH1; (c) PL decay from the wide well after excitation of the transition CB'1-LH'1. Solid lines correspond to fits according to the model described in Sec. II.

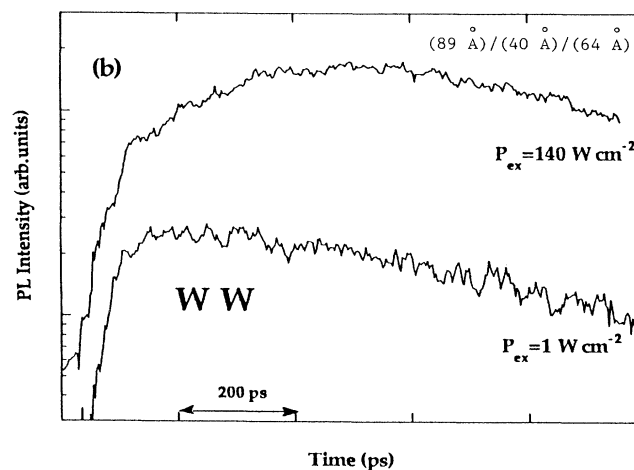
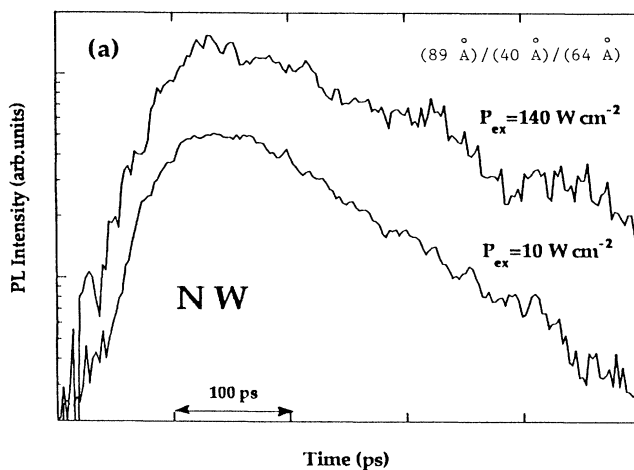


FIG. 4. PL decay curves of sample $(89 \text{ \AA})/(40 \text{ \AA})/(64 \text{ \AA})$ for different excitation intensities: (a) PL decay curves from the narrow well; (b) PL decay curves from the wide well after excitation of the transition CB'1-LH'1.

solely seems to indicate that both effects (band bending and band filling) are only important for hole dynamics. In fact a rough estimate of band bending leads to a value of a few meV, much less than the electronic mismatch ΔE_e , which is larger than 20 meV in all the samples investigated. On the contrary, this value is comparable with the energy mismatch ΔE_h between hole states in our samples. The two different rise times observed in Fig. 4(b) for the decay at high intensity could, therefore, be connected to a fast transfer of electrons and holes, followed by a slowing down of hole tunneling due to band filling of the hole levels in the wide well.

We will limit our discussion to the experimental data at the lowest intensity. Electron- and hole-tunneling times are extracted from the experimental decay curves assuming a simple model for the carrier dynamics inside the ADQW structure.

Let us consider again Fig. 1. Denoting with n_N^e (n_N^h) and n_W^e (n_W^h) the number of electrons (holes) at time t in the lowest energy level of the conduction and valence bands of the narrow and wide wells, respectively, and considering only excitonic recombination, the PL intensity from the narrow well (wide well) is proportional to the smaller of the carrier densities n_N^e and n_N^h (n_W^e and n_W^h). For example, under the usual assumption that electrons tunnel faster than holes, the excitonic recombination is governed by n_N^e in the narrow well and by n_W^h in the wide well.

A simple set of rate equations can then be written as follows:

$$\frac{dn_N^e}{dt} = -\frac{n_N^e}{\tau_N} - \frac{n_N^e}{\tau_t^e}, \quad \frac{dn_N^h}{dt} = -\frac{n_N^h}{\tau_N} - \frac{n_N^h}{\tau_t^h}, \quad (1)$$

$$\frac{dn_W^e}{dt} = -\frac{n_W^e}{\tau_W} + \frac{n_N^e}{\tau_t^e}, \quad \frac{dn_W^h}{dt} = -\frac{n_W^h}{\tau_W} + \frac{n_N^h}{\tau_t^h}, \quad (2)$$

where τ_i ($i=N, W$), τ_t^e, τ_t^h are the recombination times of the isolated wells and the electron- and hole-tunneling times, respectively.

Equations (1) and (2) can be integrated under the conditions $n_N(t=0) = n_N^0$ and $n_W(t=0) = n_W^0$, as provided by a δ -like excitation at $t=0$, to yield for the quantities of interest:

$$\begin{aligned} n_N^e &= n_N^0 e^{-t/\tau_L}, \\ n_W^h &= n_W^0 e^{-t/\tau_W} + n_N^0 \frac{\tau_{Wt}^h}{\tau_t^h} (e^{-t/\tau_t^h} - e^{-t/\tau_W}) \\ &\quad + n_N^0 \frac{\tau_{et}^h}{\tau_N \tau_t^h} [\tau_{Wt}^h (e^{-t/\tau_t^h} - e^{-t/\tau_W}) \\ &\quad - \tau_{LW} (e^{-t/\tau_L} - e^{-t/\tau_W})], \end{aligned} \quad (4)$$

where

$$\begin{aligned} \tau_L &= \frac{\tau_t^e \tau_N}{\tau_N + \tau_t^e}, \quad \tau_{et}^h = \frac{\tau_t^h \tau_L}{\tau_L - \tau_t^h}, \\ \tau_{Wt}^h &= \frac{\tau_t^h \tau_W}{\tau_t^h - \tau_W}, \quad \tau_{LW} = \frac{\tau_L \tau_W}{\tau_L - \tau_W}. \end{aligned}$$

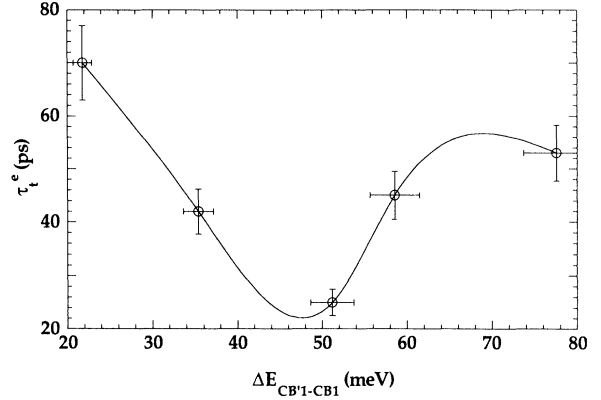


FIG. 5. Electron-tunneling time as a function of the energy mismatch ΔE between the ground electronic level CB'1 in the narrow well and the ground electronic level CB1 in the wide well for samples having the same barrier thickness. The solid line is only a guide for the eye.

Assuming τ_t^e much smaller than all other times involved, Eq. (4) reduces to

$$n_W^h = n_W^0 e^{-t/\tau_W} + n_N^0 \frac{\tau_{Wt}^h}{\tau_t^h} (e^{-t/\tau_t^h} - e^{-t/\tau_W}). \quad (5)$$

As reported in detail in a previous paper,²¹ typical excitonic recombination times in GaAs/Al_{0.3}Ga_{0.7}As quantum wells at 4 K are of the order of 200–300 ps. Since the measured PL decay times from the narrow well range from 20 to 140 ps, we can determine τ_t^e from the PL decay time at energy CB'1-HH'1 at least as long as $\tau_t^e \ll \tau_N$. For a large barrier width where τ_t^e and τ_N are of the same order of magnitude, the value we get in this way for the tunneling time should be considered as a lower limit to its real value.

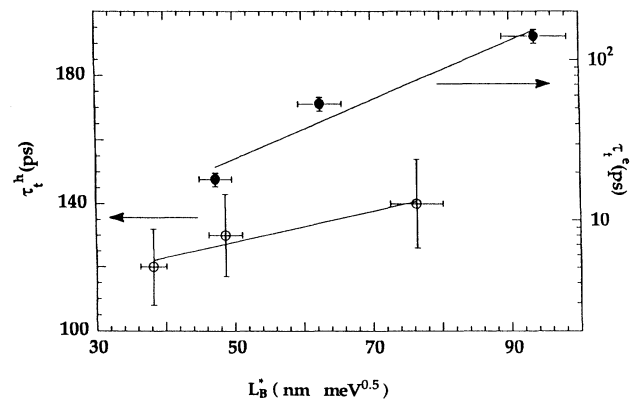


FIG. 6. Hole-tunneling time as a function of the normalized barrier thickness L_B^* for samples having the same narrow-(40 Å) and wide-well (100 Å) thicknesses (open circles); the solid line is only a guide for the eye. For comparison the electron-tunneling times for the same set of samples are reported as solid circles; the solid line corresponds to an exponential fit.

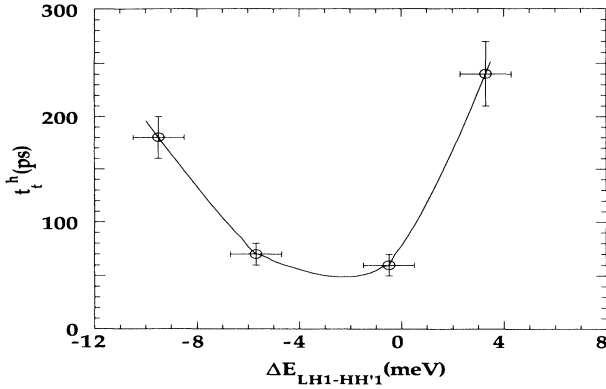


FIG. 7. Hole-tunneling time as a function of the energy mismatch ΔE at $k_{\parallel}=0$ between the first light-hole state LH1 in the wide well and the first heavy-hole state HH'1 in the narrow well for samples having the same barrier thickness. The solid line is only a guide for the eye.

The recombination time τ_W can be directly determined from the PL decay curve when only the wide well is excited, i.e., for resonant excitation of the transition CB1-LH1.

Finally τ_t^h is determined by fitting the PL decay curves from the wide well when both wells are excited. In fact τ_t^h turns out to be the only adjustable parameter in Eq. (5), being n_N^0/n_W^0 estimated directly from the PLE spectra.

To summarize, a fit to the three different decay curves corresponding to the recombination at CB'1-HH'1 and CB1-HH1 after excitation of both wells or of the wide well alone allows us to determine the unknown parameters in the rate equations (3) and (5).

The fits to the experimental data, using Eqs. (3) and (5), correspond to the solid lines in Fig. 3; the best-fit values for the tunneling times, as a function of the energy mismatch between the levels involved in the process, are reported in Figs. 5–7.

III. DISCUSSION

A. Dependence of τ_t^e on ΔE_e

We refer to Ref. 17 for a discussion of the dependence of τ_t^e on the barrier thickness L_B .

Here we shall limit the discussion to the dependence of τ_t^e on the energy mismatch ΔE_e between the ground electronic levels of the two wells for a given barrier thickness as reported in Fig. 5. It must be noted that a clear resonance in the tunneling time is observed when ΔE_e is of the order of 50 meV. Our results are in good agreement with the measurements of Oberli *et al.*²² who find a resonance in the electron-tunneling time when ΔE_e is equal to 48 meV, as in our case. Note that the broad minimum in the tunneling time occurring around $\Delta E_e \approx 50$ meV could suggest that AlAs-like LO phonons ($\text{Al}_{0.3}\text{Ga}_{0.7}\text{As}$ $E_{\text{LO}} = 48$ meV) of the barrier play an important role in assisting the tunneling process. This result is not yet clearly

understood. On one hand, due to the fact that the electron wave function is mainly localized in the wells, one would expect a major role played by the GaAs LO phonon at 36 meV; on the other hand, if one considers scattering processes occurring in the barrier, two resonances should be observed, one associated to the GaAs-like phonon and the other to the AlAs-like phonon. Our experimental findings seem to indicate that tunneling is preferentially assisted by scattering events in the barrier, given the shift towards the AlAs-like phonon energy. At the same time, to our knowledge, no mechanism has been proposed for the electron-phonon interaction which might privilege, in the tunneling process, the coupling with the AlAs phonon. It must also be noted that the increase of τ_t^e for $\Delta E_e \geq 50$ meV might be due to less efficient scattering processes due to a reduced Fröhlich interaction, and we should expect a further decrease in the electron-tunneling time as soon as ΔE_e becomes larger than twice the phonon energy.

B. Dependence of τ_t^h on ΔE_h

We report, in Fig. 6, the hole-tunneling time τ_t^h for samples having the same thicknesses of the wide and narrow well, 100 and 40 Å, respectively, as a function of the normalized barrier thickness²³ L_B^* , defined as

$$L_B^* = \left[\frac{m_{\text{barrier}}}{m_{\text{well}}} (V - E) \right]^{1/2},$$

where L_B is the barrier thickness, m is the effective mass of the carrier, V is the barrier height, and E the energy of the carrier. As a comparison, it is also reported in Fig. 6 the dependence of the electron-tunneling time on L_B^* for the same set of samples.

While in the case of electrons we find an exponential dependence of the tunneling time on L_B^* in agreement with similar results from other authors,¹⁰ the hole-tunneling time turns out to be mildly dependent on the barrier thickness in the range 30–70 Å.

We want to remark that fast hole tunneling ($\tau_t^h \approx 100$ ps) has also been found, by other authors,¹³ in samples with near-resonant states in valence bands as in our case ($\Delta E_h \approx 2$ meV at $k_{\parallel}=0$), but no observation of a weak dependence of the tunneling time on the barrier thickness, to our knowledge, has been reported.

This result is quite surprising if compared with what is found for electrons where, even in resonance conditions, an exponential behavior of the tunneling time is measured when the barrier width is larger than 40 Å.¹⁰ While it is clear that band alignment in the valence band can originate fast hole tunneling, further investigation is needed in order to understand the observed weak dependence of the tunneling time on L_B , especially when L_B is as large as 70 Å and no hybridization between the hole wave functions in the two wells seems to occur. Nevertheless, due to the fast electron tunneling, the establishment of a space charge and therefore a band bending comparable with the energy separation between the hole

levels involved in the tunneling process (a few meV) could strongly influence the hole tunneling and make it easier. Note that the opposite situation occurs in the presence of an electronic resonance; in this case the band bending produced by the photogenerated space charge would oppose an electron resonant transfer.

The hole-tunneling time τ_t^h is reported in Fig. 7 as a function of the energy mismatch ΔE_h between heavy- and light-hole states at $k_{\parallel}=0$ in the ADQW structures investigated. A significant reduction of the hole-tunneling time is observed as soon as the energy mismatch between the first light-hole state LH1 in the wide well and the first heavy-hole state HH'1 in the narrow well decreases to less than a few meV. Since the two levels are decoupled at $k_{\parallel}=0$, the reduction in the tunneling time should be associated to a resonance induced by band-mixing effects at $k_{\parallel} \neq 0$.

In Figs. 8(a) and 9(a) we show the calculated hole level dispersion as a function of k_{\parallel} for the samples $(88 \text{ \AA})/(38 \text{ \AA})/(45 \text{ \AA})$ and $(92 \text{ \AA})/(38 \text{ \AA})/(56 \text{ \AA})$ for which short (≈ 60 – 70 ps) hole-tunneling times are observed. The calculation is done using a numerical solution of the Luttinger Hamiltonian based on the finite-difference method.²⁴ The dispersion of the coupled ADQW is superimposed onto the hole dispersions of the isolated quantum wells. It can be seen that the ADQW dispersion parallels those of the isolated quantum wells up to the point where they come close to each other and anticrossing occurs.²⁵ Only then the wave function of the coupled

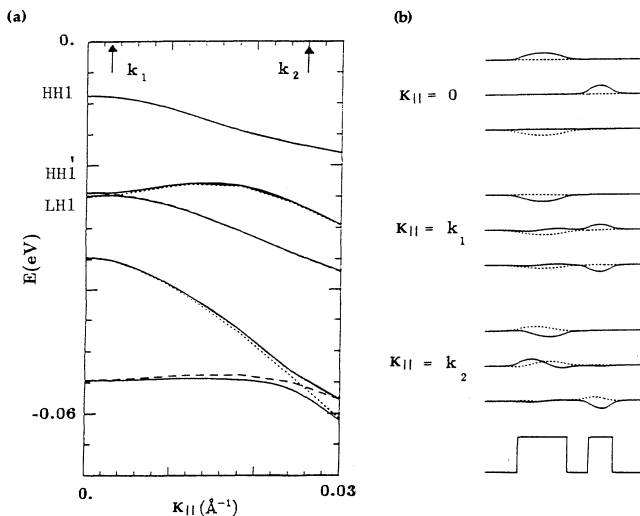


FIG. 8. (a) Valence-band dispersion of the ADQW $(88 \text{ \AA})/(38 \text{ \AA})/(45 \text{ \AA})$ (solid line) and the isolated 88 \AA (dotted line) and 45 \AA QW's (dashed line) as a function of the in-plane momentum. The values k_1, k_2 for which the eigenfunctions are shown are indicated by an arrow. (b) Eigenfunctions of the first three ADQW states at three values of k_{\parallel} ; heavy-hole component, solid line; light-hole component, dotted line. At $k_{\parallel}=k_1$, where anticrossing occurs, the second and third levels are extended to the whole ADQW structure for which the potential profile is shown at the bottom.

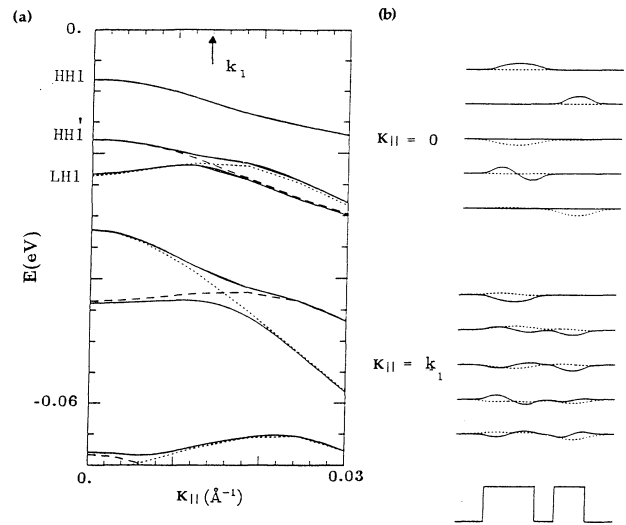


FIG. 9. (a) Valence-band dispersion of the ADQW $(92 \text{ \AA})/(38 \text{ \AA})/(56 \text{ \AA})$ (solid line) and the isolated 92 \AA (dotted line) and 56 \AA QW's (dashed line) as a function of the in-plane momentum. The value k_1 for which the eigenfunctions are shown is indicated by an arrow. (b) Eigenfunctions of the first five ADQW states at two values of k_{\parallel} ; heavy-hole component, solid line; light-hole component, dotted line. At $k_{\parallel}=k_1$, where anticrossing between second and third and fourth and fifth level occurs, the eigenfunctions are extended to the whole ADQW structure for which the potential profile is shown at the bottom.

system becomes extended over both wells as shown in Figs. 8(b) and 9(b). In particular, if we focus on the second level of Fig. 8(a), which is a pure heavy-hole state localized in the NW at $k_{\parallel}=0$ [see Fig 8(b)], we see how the second level hybridizes with the level originating from LH1 at the value of k_{\parallel} where anticrossing occurs and eventually becomes a mixed heavy–light-hole state, completely localized in the WW, at larger k_{\parallel} 's. This im-

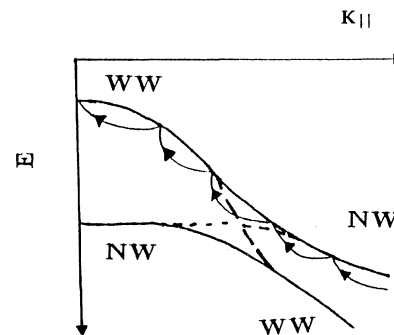


FIG. 10. Schematic picture of the ADQW levels (solid line) resulting from anticrossing of levels localized in the WW (dashed line) and NW (dotted line). A sketch of the relaxation path to $k=0$ of a carrier excited into the NW at k_{\parallel} greater than that for which anticrossing occurs is shown. The charge is transferred from the NW to the WW during intraband relaxation.

plies that a hole created in the narrow well can be transferred to the wide well via fast intraband relaxation as sketched in Fig. 10. The qualitative picture presented could account for the very different hole-tunneling times observed for structures where anticrossing between heavy- and light-hole states occurs or not. Furthermore this charge-transfer mechanism should not be particularly sensitive to the effect of a small band bending, which would just shift the value of k_{\parallel} where anticrossing occurs. We also want to remark that the minimum observed in the hole-tunneling time for the sample that shows an anticrossing at $k_{\parallel} \approx 0$ agrees with the proposed mechanism for the hole tunneling. In fact, due to the resonant excitation, fast transfer should be favored when hybridization occurs near the Γ point.

We believe that our results give clear evidence of fast tunneling due to resonant states in the valence band. The observed reduction of the hole tunneling in presence of resonances between heavy and light levels is in good agreement with the calculations of Ferreira and Bastard.¹¹ Moreover, from a comparison of the values of τ_i^h reported in Figs. 6 and 7, faster escape constants are found for holes when anticrossing between heavy and light levels is present. This could be explained, in agreement with recent results on exciton thermalization,²⁶ if one considers tunneling processes occurring during the thermalization path whenever a coupling between the relevant states is possible at $k_{\parallel} \neq 0$ (Fig. 10). It should also be noted that resonances associated with band mix-

ing are broader than resonances between heavy-hole states¹¹ and, therefore, they might be easier to reach in unbiased samples.

SUMMARY

Resonance effects in the tunneling time of the carriers photogenerated in ADQW structures by picosecond laser pulses have been investigated.

Referring to the electron-tunneling time, our data show a clear resonance associated with phonon-assisted processes at an energy comparable with the AlAs-like LO phonon, suggesting an important role played by scattering events in the barrier.

Significant shortening in the hole-tunneling time is found both in the case of resonances between heavy-hole states and when resonances are due to mixing between heavy- and light-hole levels, in good agreement with recent calculations of the hole-tunneling times.

ACKNOWLEDGMENTS

We thank M. G. W. Alexander, G. Bastard, F. Capasso, M. Gurioli, P. Lugli, and E. Molinari for helpful discussions and C. Deparis, J. Massies, and G. Neu for providing the samples. One of us (Ph.R.) thanks Centre National de la Recherche Scientifique (CNRS) for financial support. The Università degli Studi di Firenze is affiliated with the Gruppo Nazionale di Struttura della Materia and the Consorzio Interuniversitario di Struttura della Materia.

*Permanent address: Laboratoire d'Optique Quantique du Centre National de la Recherche Scientifique, Ecole Polytechnique, 91128 Palaiseau CEDEX, France.

¹L. Esaki and R. Tsu, IBM J. Res. Dev. **14**, 61 (1970).

²R. Tsu and L. Esaki, Appl. Phys. Lett. **22**, 562 (1973).

³L. L. Chang, L. Esaki, and R. Tsu, Appl. Phys. Lett. **24**, 593 (1974).

⁴D. Y. Oberli, J. Shah, T. C. Damen, C. W. Tu, T. Y. Chang, D. A. B. Miller, J. E. Henry, R. F. Kopf, N. Sauer, and A. E. Di Giovanni, Phys. Rev. B **40**, 3028 (1989).

⁵M. G. W. Alexander, W. W. Ruhle, R. Sauer, and W. T. Tsang, Appl. Phys. Lett. **55**, 885 (1989).

⁶B. Deveaud, F. Clerot, A. Chomette, A. Regreny, R. Ferreira, G. Bastard, and B. Sermage, Europhys. Lett. **11**, 367 (1990).

⁷M. Nido, M. G. W. Alexander, W. W. Ruhle, T. Schweizer, and K. Kohler, Appl. Phys. Lett. **56**, 355 (1990).

⁸M. G. W. Alexander, M. Nido, W. W. Ruhle, and K. Kohler, Phys. Rev. B **41**, 12 295 (1990).

⁹T. Matsusue, M. Tsuchiya, J. N. Schulman, and H. Sakaki, Phys. Rev. B **42**, 5719 (1990).

¹⁰B. Deveaud, A. Chomette, F. Clerot, P. Auvray, A. Regreny, R. Ferreira, and G. Bastard, Phys. Rev. B **42**, 7021 (1990).

¹¹R. Ferreira and G. Bastard, Europhys. Lett. **10**, 279 (1989).

¹²K. Leo, J. Shah, J. P. Gordon, T. C. Damen, D. A. B. Miller, C. W. Tu, and J. E. Cunningham, Phys. Rev. B **42**, 7065 (1990).

¹³M. Nido, M. G. W. Alexander, W. W. Ruhle, and K. Kohler, Phys. Rev. B **43**, 1839 (1991).

¹⁴R. Sauer, K. Thonke, and W. T. Tsang, Phys. Rev. Lett. **61**, 609 (1988).

¹⁵T. B. Norris, N. Vodjdani, B. Vinter, C. Weisbuch, and G. A.

Mourou, Phys. Rev. B **40**, 1392 (1989).

¹⁶R. Ferreira, C. Delalande, H. W. Liu, G. Bastard, B. Etienne, and J. F. Palmier, Phys. Rev. B **42**, 9170 (1990).

¹⁷Ph. Roussignol, M. Gurioli, L. Carraresi, M. Colocci, A. Vinattieri, C. Deparis, J. Massies, and G. Neu, Superlatt. Microstruct. **9**, 151 (1991).

¹⁸See, for instance, G. Bastard, *Wave Mechanics Applied to Semiconductor Heterostructures* (Les Edition de Physique, Les Veis, 1988).

¹⁹L. C. Andreani, and A. Pasquarello, Phys. Rev. B **42**, 8928 (1990).

²⁰K. Leo, J. Shah, E. Gobel, T. C. Damen, K. Kohler, and P. Ganser, Superlatt. Microstruct. **7**, 427 (1990).

²¹M. Colocci, M. Gurioli, A. Vinattieri, F. Fermi, C. Deparis, J. Massies, and G. Neu, Europhys. Lett. **12**, 417 (1990); M. Gurioli, A. Vinattieri, M. Colocci, C. Deparis, J. Massies, G. Neu, A. Bosacchi, and S. Franchi, Phys. Rev. B **44**, 3115 (1991).

²²D. Y. Oberli, J. Shah, T. C. Damen, J. M. Kuo, J. E. Henry, J. Lary, and S. M. Goodnick, Appl. Phys. Lett. **56**, 1239 (1990).

²³Calculations of the normalized barrier thickness have been done using the parameter values reported in Ref. 19.

²⁴A. Fasolino and M. Altarelli, in *Band Structure Engineering in Semiconductor Microstructures*, edited by R. A. Abram and M. Jaros (Plenum, New York, 1989), p. 367.

²⁵We recall that level crossing at $k_{\parallel} = 0$ is forbidden by symmetry also in the isolated QW's, giving rise to the strongly non-parabolic hole-subband dispersion displayed in Figs. 8(a) and 9(a).

²⁶T. C. Damen, J. Shah, D. Y. Oberli, D. S. Chemla, J. E. Cunningham, and J. M. Kuo, Phys. Rev. B **42**, 7434 (1990).